인지과학, 제29권 제3호
Korean Journal of Cognitive Science
2018, Vol. 29, No. 3, 161～192.
http://dx.doi.org/10.19066/cogsci.2018.29.3.001

Interactivity within large-scale brain network recruited for retrieval of temporally organized events*

Yoonjin Nah[1)*] Jonghyun Lee[2)*] Sanghoon Han[1),2)]

[1)]Department of Psychology, Yonsei University
[2)]Graduate Program in Cognitive Science, Yonsei University

Retrieving temporal information of encoded events is one of the core control processes in episodic memory. Despite much prior neuroimaging research on episodic retrieval, little is known about how large-scale connectivity patterns are involved in the retrieval of sequentially organized episodes. Task-related functional connectivity multivariate pattern analysis was used to distinguish the different sequential retrieval. In this study, participants performed temporal episodic memory tasks in which they were required to retrieve the encoded items in either the forward or backward direction. While separately parsed local networks did not yield substantial efficiency in classification performance, the large-scale patterns of interactivity across the cortical and sub-cortical brain regions implicated in both the cognitive control of memory and goal-directed cognitive processes encompassing lateral and medial prefrontal regions, inferior parietal lobules, middle temporal gyrus, and caudate yielded high discriminative power in classification of temporal retrieval processes. These findings demonstrate that mnemonic control processes across cortical and subcortical regions are recruited to re-experience temporally-linked series of memoranda in episodic memory and are mirrored in the qualitatively distinct global network patterns of functional connectivity.

Key words : Controlled retrieval, Functional connectivity multivariate pattern analysis, temporal episodic memory

---

* This research was supported by the Brain Research Program through the National Research Foundation of Korea(NRF) funded by the Ministry of Science, ICT & Future Planning (NRF-2017M3C7A1029688).

† 교신저자: Sanghoon Han
연구 분야: Memory, Functional neuroimaging
E-mail: sanghoon.han@yonsei.ac.kr

Introduction

Episodic memory encompasses vast amounts of information including time, place, and self-referential content, and the memories are tagged to each event allowing the retrieval of past events (Tulving, 2002). Of particular importance is the ability to mentally go back and forth in time and re-experience sequentially organized memory events being the key controlled processes in human cognition (Tulving, 1972, 1983). Although it has long been suggested that complex mechanisms, such as executive function, planning, and visuospatial processing, play important roles in sequential temporal memory processes (Lezak, 1995; Schofield & Ashman, 1986), how the brain networks are involved is yet to be investigated.

Prior behavioral and clinical research has utilized the sequential retrieval manipulation to assess response time and performance accuracy as indicators of cognitive control ability (Anders & Lillyquist, 1971; Drosopoulos, Windau, Wagner, & Born, 2007; Kahana & Caplan, 2002; Thomas, Milner, & Haberlandt, 2003). While participants can retrieve a relevant memory target that follows the presented cue item by using the directional flow or causality of encoding contexts (forward), the reverse may require participants to cognitively travel back from the cue item and search for the target in their long-term memory. Under such circumstances, goal-relevant targets cannot be automatically driven simply by encoding cues; thus, top-down processing such as controlled retrieval is essential for backward retrieval. For this matter, temporal memory task, especially sequential processing in reverse order of memoranda, has been frequently examined in several neuropsychological tests (i.e., Digit Span Backward from the Wechsler Adult Intelligence Scale; Wechsler, 2008) and the task has also been investigated as one of the most clinically important cognitive domains in various groups such as Alzheimer's dementia (Storandt, Kaskie, & Von Dras, 1998), Parkinson's disease cognitive impairment (Sagar, Sullivan, Gabrieli, Corkin, & Growdon, 1988; Vriezen & Moscovitch, 1990), preclinical Huntington's disease (Pirogovsky, et al., 2009), amnesic patients (Bowers, Verfaellie, Valenstein, & Heilman, 1988), patients with selective hippocampal lesions (Mayes et al., 2001) as well as in the normal elderly participants (Fabiani & Friedman, 1997; Parkin, Walter, & Hunkin, 1995).

These laboratory and neuropsychological behavioral studies have shown the presence of backward-retrieval detriment or forward-retrieval advantage mediated by the differential controlled process involved in the different directions of sequential retrieval (Anders & Lillyquist, 1971; Drosopoulos, Windau, Wagner, & Born, 2007; Thomas, Milner, & Haberlandt, 2003). However, the

underlying neural patterns of the brain involved in the sequential retrieval processes and how the controlled process is differentially recruited in these two directions are yet to be fully discussed. Given the various cognitive processes involved, we assumed that controlled retrieval of sequentially encoded events would be achieved by global brain networks and its interactivity among control network regions. However, little research has reported the differential neural network patterns, especially regarding how interactivity within large-scale brain network is recruited for retrieval of temporally organized events.

Previous univariate functional magnetic resonance imaging (fMRI) analyses (e.g., statistical parametric mapping) of blood oxygen level-dependent (BOLD) activity have demonstrated that the left ventrolateral prefrontal cortex (VLPFC), specifically the anterior part (aVLPFC; Brodmann area (BA) 47, the pars orbitalis subarea of the inferior frontal gyrus), play a crucial role in cognitively controlled retrieval processes (see Badre & Wagner, 2007 for a review), such as controlled retrieval of semantic memories (Badre, Poldrack, Pare-Blagoev, Insler, & Wagner, 2005; Han, O'Connor, Eslick, & Dobbins, 2012; Wagner, Pare-Blagoev, Clark, & Poldrack, 2001) and retrieval of contextual information (Dobbins & Han, 2006; Raposo, Han, & Dobbins, 2009). These findings shed lights on the understanding of neural substrates for controlled retrieval; however, the localizing brain activity typically relies on the mass-univariate methods (i.e., statistical parametric mapping) based on the assumption that different brain regions function in independent (voxel-level) manners.

Recently, there is increasing evidence that the left aVLPFC functionally couples with several cortical as well as sub-cortical brain regions. For example, Neubert, Mars, Thomas, Sallet, and Rushworth (2014) observed that during the resting-state period, aVLPFC (BA 47) is connected with several brain regions, including other prefrontal sub-areas, the temporal, parietal, and premotor cortices. Similarly, Han, et al. (2012) also found that the left VLPFC is intrinsically connected with both cortical and subcortical areas, including the bilateral PFC, middle temporal gyrus, parietal, and caudate regions. Recently, functional connectivity findings from task-based fMRI study has also shown similar functional coupling patterns in intrinsically defined networks, such as the inferior parietal, temporal, and striatal regions (Barredo, Oztekin, & Badre, 2015). The results also demonstrated that the left aVLPFC was functionally connected with other large-scale brain networks, such as the frontoparietal control network (Spreng, Stevens, Chamberlain, Gilmore, & Schacter, 2010; Vincent, Kahn, Snyder, Raichle, & Buckner, 2008), which has been suggested to play a crucial role in the cognitive control processes (Badre & D'Esposito, 2007; Cabeza, Ciaramelli, Olson, & Moscovitch, 2008; Corbetta, Patel, &

Shulman, 2008; Koechlin, Basso, Pietrini, Panzer, & Grafman, 1999). Taken together, these connectionism approaches provide a basis for identifying the potentially relevant nodes and raise the possibility that interregional and integrative functional connectivity multivariate patterns across distributed cortical and sub-cortical regions are involved in the sequential retrieval of temporally organized events.

The purpose of this study was two-fold. First, we aimed to assess whether multivariate patterns of brain connectivity were distinguishably employed for the retrieval processes of sequentially organized events either in the forward or backward direction. We used a machine learning algorithm (Cortes & Vapnik, 1995; Vapnik, 1999) and the novel approach adopted in the current study was that we applied a task-based functional connectivity multivariate pattern analysis (fcMVPA) approach with task-related time-series extracted in a voxel-wise manner from the whole brain. If sequential retrieval in different directions would demand differential controlled processes based on distinctive networks, the task-based functional connectivity patterns obtained from the sequential retrieval period can be used to discriminate the forward and backward retrieval processes. To identify the most optimally distinctive network patterns, we also employed iterative search methods for classification as a function of the number of input features included (Pantazatos, Talati, Pavlidis, & Hirsch, 2012a, 2012b; Pantazatos, Talati, Schneier, & Hirsch, 2014).

Next, the current experiment also specifically aimed to collectively elucidate the whole-brain pattern characteristics of networks and to address how these are related to the regions previously implicated in controlled retrieval regions. We compared the achieved pattern classification performance across separately parsed networks to reveal whether our discriminating features (i.e., connectivity pattern) encompass the whole brain or are only restricted to within local networks (i.e., lateral prefrontal, parietal, temporal, striatal, fronto-parietal, fronto-temporal, fronto-striatal regions). Identification of distinctive whole-brain connectivity features would provide more thorough insights into how the mnemonic control processes to re-experience temporally-linked series of memoranda in episodic memory is represented in the brain.

Materials and Methods

Participants

Twenty-two healthy volunteers (8 females; mean age = 23.23, *SD* = 2.39) participated in the experiment and were paid for their time (10,000 South Korean Won/hour). Two participants were excluded from all analyses because of incompletion due to fatigue, and the analysis for the N-back task was conducted with data from only 19 participants because data for one participant were unavailable. All participants had normal or corrected-to-normal vision and were right-handed. Informed consent was obtained in a manner approved by the Institutional Review Board of Yonsei University. Prior to the experiment, participants were screened for any significant medical conditions, including their history of neurological or psychiatric diagnoses.

Experimental Materials and Procedures

The current fMRI study included a simplified temporal episodic memory task and one working memory task (N-back) (Fig. 1). Prior to the actual task runs, resting-state data were collected to discover intrinsic functional connectivity. During resting-state data acquisition, participants were instructed to close their eyes while lying awake and to not think of anything in particular or in a systematic way. After resting-state data collection, the actual experimental runs began. The temporal episodic memory task consisted of an encoding and a retrieval runs. The experimental items of the episodic memory task were composed of 90 and 160 common Korean nouns (2 syllable words with 2 Korean letters long). All word items were projected onto a screen with a black background and viewed using a mirror mounted on the head coil. Before starting the actual fMRI scanning experiment runs, participants completed a practice run outside of the scanner using a laptop computer. Both the practice and experimental trials were programmed using the Cogent 2000 toolbox (www.vislab.ucl.ac.uk/cogent.php) and MATLAB 7.12.0 (The MathWorks, Natick, MA).

During the encoding run of temporal memory task, participants were asked to memorize triplets of words (e.g., A–B–C) and each word was presented sequentially for 2 s at the center of the screen. Each trial was followed by an association period for another 8 s, during which the participants were required to mentally make associations with the word triplet in sequence. The encoding run included

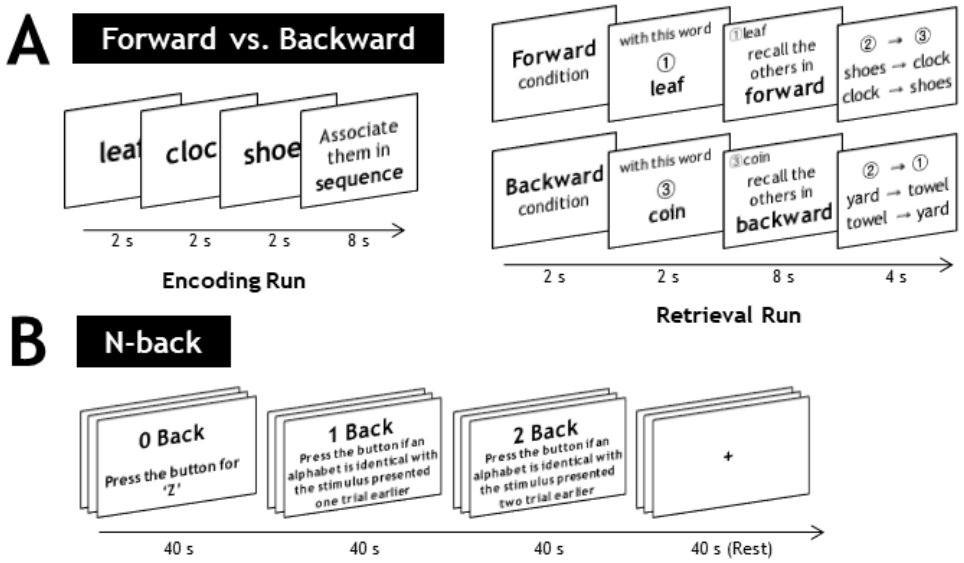

(Figure 1) Schematic figure of the experimental paradigm and stimuli examples. (A) A series of word triplets were successively presented during the encoding run. The retrieval run consisted of two different conditions. Participants were required to retrieve the other two words in sequential order in the forward or backward direction. (B) The N-back working memory task consisted of three different conditions (i.e., 0-back, 1-back, and 2-back) in a block design, followed by a mini-resting block

30 trials (triplets) for a total of 90 words. In the retrieval run, directional instruction (i.e., forward or backward) for each trial was shown for 2 s, then either the first or last word of a triplet (A or C) learned in the encoding run was presented as a cue for 2 s. During the next 8 s, participants were required to rehearse the other two words in sequential order (forward retrieval; A–B–C) or in the backward direction (backward retrieval; C–B–A). Finally, participants had another 4 s to choose the correct answer from two options (in forward retrieval, B–C versus C–B; in backward retrieval, A–B versus B–A), and the order of the two options was randomized. The retrieval run consisted of 30 trials of alternating mini-blocks of the forward and backward conditions, and each mini-block included five trials.

After completing the temporal memory task, participants performed a working memory task, N-back, during which they were successively presented with a series of single-alphabet letters. The working memory task is employed to ensure that the expected sequential memory activation does not merely result from the working memory load difference but rather from the demand required for

controlled retrieval processes. The N-back task included a total of three conditions (0-back, 1-back, and 2-back) in a block design. In the 0-back condition, the target was the letter "Z" and participants pressed a button as quickly as possible whenever the letter on the screen matched the target. In the 1-back and 2-back conditions, participants responded if the letter on the screen was identical to the stimulus presented one trial or two trials earlier, respectively. Each condition block consisted of 19 trials and there were four target trials in a block. One cycle was composed of three condition blocks and one mini-resting block, and each cycle was repeated three times in the same order.

fMRI Data Acquisition

Neuroimaging data were acquired with the 3T General Electric Healthcare Discovery MR750 (Waukesha, WI) using an 8-channel radiofrequency head coil. Functional data were obtained with a T2*-weighted gradient-echo echoplanar imaging sequence (TR = 2000 ms, TE = 30 ms, 3.75 × 3.75 × 4.0 mm^3 in-plane resolution, 33 axial slices tilted 30° from the AC–PC plane to reduce the influence of in-plane susceptibility gradients (Deichmann, Gottfried, Hutton, & Turner, 2003), no gap, and interleaved collection). The first five volumes of each run were discarded prior to the actual data collection to ensure magnetization equilibrium. For the temporal memory task, 210 and 270 volumes were collected for the encoding and retrieval runs, respectively. In addition, 260 volumes were collected for the N-back run. Resting-state MRI data were collected prior to the experimental runs (204 volumes). Participants responded with a magnet-compatible button box placed under the right hand. At the end of the functional imaging runs, 3-dimensional T1-weighted structural images (TR = 8.28 ms, TE = 3.29 ms, FOV = 198 × 220 mm^2, voxel size = 0.77 × 0.86 × 1.0 mm^3, 216 sagittal slices, flip angle = 12°, and no gap) were acquired for visualization.

Functional Data Preprocessing and Analyses

Preprocessing and general linear model (GLM) analyses were conducted using SPM8 (Wellcome Department of Cognitive Neurology, London, U.K.) that includes for all task-evoked responses and a nuisance covariate, the run effect regressor. A slice-timing correction was accomplished by resampling all slices relative to the middle slice. Functional images were then realigned to the first volume for

motion correction, spatially normalized to the Montreal Neurological Institute (MNI) template provided with SPM8, then resampled into 3 × 3 × 3 mm^3 size voxels, followed by spatial smoothing using a Gaussian kernel with a full width at a half maximum of 8 mm. We focused on the retrieval runs since we were investigating the differences in neural processes between the forward and backward retrieval directions.

All volumes of each run were treated as temporally correlated time-series and modeled by convolving a canonical hemodynamic response function (HRF) and its temporal derivative (except there was no temporal derivative for N-back due to the block design). The resulting hemodynamic functions were used as covariates in GLM, along with a covariate for the run effect. A high-pass filter (cut off 128 s) was applied to remove low-frequency trends, and an autoregressive AR(1) model + white noise correction was used to estimate and correct for non-sphericity of the error covariance (Friston, et al., 2002). The least-square parameter estimates of the best-fitting synthetic HRF for each condition of interest were used in pair-wise contrasts and stored as separate images for each participant; these were then checked against the null hypothesis with one-tailed *t*-tests to determine whether effects of participants were random at the group level. Given that the primary aim of the current study is to conduct fcMVPA, GLM analyses adopted less stringent uncorrected threshold to explore sufficient number of potential node regions. Clusters consisting of five or more contiguous voxels (3 mm isotropic) with $p < .001$ were chosen to be considered significant.

Resting-State Data Preprocessing and Analysis

Resting-state data were preprocessed using a Data Processing Assistant for Resting-State fMRI (Yan & Zang, 2010) which was developed based on SPM8 and the Resting-State fMRI Data Analysis Toolkit (Song, et al., 2011). For slice-timing correction, realignment, normalization, and smoothing processes of resting-state data, we followed the same protocols as those used for preprocessing of functional data described above. Subsequently, data were detrended and temporally filtered with a low-pass band filter (0.01–0.08 Hz). Furthermore, nuisance covariates including six head motion parameters, global mean signal, white matter signal, and cerebrospinal fluid signal were regressed out to improve the validity of our findings. Seed-to-voxel connectivity maps were generated for each participant and then were entered into the group level analysis. Participants were treated as a random effect to generate node maps to further investigate task-relate functional connectivity multivariate

pattern analyses.

Functional Connectivity Multivariate Pattern Analysis

Given that pattern analysis is more sensitive to extract subtle differences from distributed multi-dimensional functional effect than is GLM, we employed multivariate pattern analysis approach based on the machine learning algorithm. The novel approach adopted in our methods was that we extracted neural time-series across the whole retrieval runs and then convolved them with psychological factors (i.e., two different retrieval directions) to generate condition-weighted time-series in a voxel-by-voxel manner and take the cross-correlation between all voxels into account. This multivariate approach also has advantages in that the researchers do not need to pre-define ROIs (i.e., seed regions in Psycho-physiological Interaction (PPI)); thus, findings are not restricted to represent bivariate (seed-to-voxels) relations, and also in that it allows us to examine a simultaneous large-scale brain network changes rather than local alternations.

Task-Related Time-Series Extraction and Node Definitions for Connectivity Analysis

To obtain task-related time-series reflecting psychological factors, BOLD signal time-series were extracted from the whole brain in a voxel-wise manner for all retrieval runs using in-house scripts in MATLAB. The extracted BOLD signal time-series were then deconvolved with a parametric empirical Bayesian formulation implemented in SPM to estimate voxel-by-voxel neural time-series, and these were detrended to remove any linear and nonlinear trends. Condition-specific psychological factors were defined by contrasting the onset time points of each retrieval condition against baseline (i.e., 1 for forward retrieval conditions and 0 for others during forward retrievals or 1 for backward retrieval conditions and 0 for others during backward retrievals). Next, condition-weighted time-series were generated separately for the two retrieval directions by multiplying the aforementioned neural time-series with psychological factors. Since the condition-weighted time-series obtained here were based on neuronal activity, the time-series were convolved again with a canonical HRF to generate signals that were more closely related to BOLD signals measured with MRI. Finally, HRF-convolved time-series were detrended.

In order to avoid any biases resulting from the node selection based on task-activated patterns such as GLM findings, the nodes for additional functional connectivity analyses were defined based on the

results of the intrinsic resting-state analysis. The seed for resting-state connectivity analysis was defined within the aVLPFC region exclusively implicated in the temporal retrieval rather than working memory process in our data (see Results section 3.2.1). The time series of seed region was extracted and was correlated with the time courses of all other voxels using the Pearson cross-correlation. The intrinsic connectivity map obtained from the resting-state analysis generated 42 peak regions based on SPM-identified whole sub-peak local maxima. Any voxels outside of the gray matter were excluded, which resulted in a total of 31 peak voxels (see Section 3.2.2). We then created cube-shaped nodes of 27 voxels (3 × 3 × 3) centered on each peak voxel. To obtain a representative time-series for each node, the first eigenvariate time-series was extracted from whole voxels of the node using the principal component analysis (PCA) function embedded in MATLAB. This generated a total of 62 task-related time-series (31 for forward and 31 for backward retrieval types) for each participant.

Iterative Multivariate Pattern Analysis

For each participant, pair-wise cross-correlation coefficients (Pearson correlation coefficient) between the time-series of whole nodes were calculated, which generated 31 × 31 symmetrical connectivity matrices. Since the resulting matrices were symmetric with respect to the diagonal, only 465 elements from the lower half of the matrix (i.e., 31 × 30/2) were used as features for further connectivity analyses. For feature selection, *t*-tests using correlation coefficients from two retrieval directions were performed for each feature comparing the differences between the means of the two conditions. Then, 465 features were ranked based on the absolute *t*-score values to eliminate any directional bias, and z-score transformation was applied to each feature (*r*) to improve normality.

To test whether patterns of functional connectivity from each retrieval direction could discriminate between different directions of retrieval processes, we conducted fcMVPA using a linear support vector machine (SVM) algorithm embedded in the Spider v1.71 MATLAB toolbox (http://people.kyb.tuebingen.mpg.de/spider/). For SVM classification, 465 elements were used as input features, and data were labeled with two different class labels for training to identify the original retrieval direction membership (i.e., 1 and -1 for forward and backward, respectively). Classification accuracies were obtained in succession as a function of a range of included features, which were arranged in descending order by their absolute *t*-score value. Specifically, the N^{th} SVM classification accuracy was obtained using the top N features, for which the *t*-score values were arranged from the highest to N^{th}. Then, the $(N+1)^{th}$ accuracy was calculated by adding an additional feature that had

the next highest *t*-score value to the feature that was already included. This process was iterated until the classification used all features, from the top feature to the last feature with the lowest *t*-score value. Therefore, this method resulted in a total of 465 accuracy measures. The purpose of this approach was not to find the algorithm that maximized the prediction accuracy. Instead, it was designed to explore which features were potentially informative in classifying different retrieval types. Furthermore, we investigated the optimal number of features needed for machine learning processes since simply including complete data features for SVM classification may result in noisy information being used to train and test the classifier.

Each SVM classification performance was estimated using a leave-one-subject-out cross validation procedure. For each iteration of the validation, one subject (one sample from the forward and another sample from the backward types) was removed and the remaining 19 subjects (thus 19 forward and 19 backward types) were put into the machine learning algorithm to train the classifier. The excluded two samples from one subject were then used to test the performance of the classifier: if the classifier predicted the class label of each test sample correctly, accuracy was scored as "1," whereas if an incorrect prediction was made, it was scored as "0." Therefore, there were 40 accuracies estimated from 20 rounds of iterations, which were then averaged to obtain one representative accuracy measure for the N^{th} SVM classification. To verify that the fcMVPA accuracies were valid, we also calculated the null distribution of 1000 permutations. For each permutation testing iteration, the original class labels were randomly shuffled and used for the SVM classification. The classification procedures occurred as conducted with the original data. If the connectivity patterns for the two retrieval directions were truly different and if each type had distinctive combinations of connectivity, randomly shuffled class labels for SVM classification should result in an accuracy of approximately 50%, whereas classification based on the original class labels should yield accuracy above chance.

Results

Behavioral Data

Accuracy (%)

Participants had better accuracy in the forward condition compared to that in the backward

condition (72% versus 62%, respectively; $t(19) = 2.36$, $p = .029$). There were no significant differences in accuracy between load conditions on the N-back task (0-back, $M = 96.49$, $SD = 1.95$; 1-back, $M = 99.12$, $SD = 0.60$; 2-back, $M = 93.86$, $SD = 2.46$), with the exception of marginal differences between 1-back and 2-back conditions ($t(18) = 1.99$, $p = .062$).

Response Time (ms)

The mean response times (RTs) in the backward condition were significantly slower than those in the forward condition (2102 ms versus 2458 ms, $t(19) = -4.46$, $p < .001$). Overall RTs in the N-back task averaged 472 ms. The 2-back condition had the slowest RTs, whereas the 1-back condition had the fastest RTs (451 ms, 419 ms, and 544 ms for 0-back, 1-back, and 2-back, respectively).

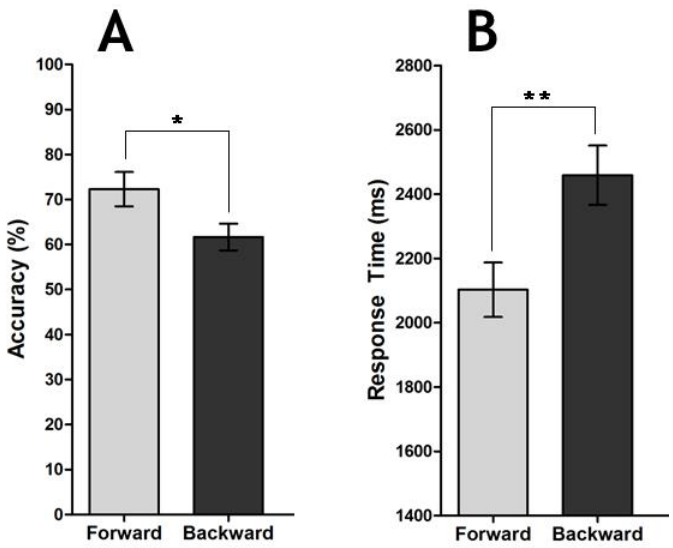

(Figure 2) Behavioral results of the mean accuracy (A) and response time (RT) (B). Error bars represent standard errors of the mean $^{*}p < .05$, $^{**}p < .001$.

Functional Neuroimaging Data

Neural Regions Associated with the Sequential Episodic Retrieval

We first calculated the contrast between forward retrieval versus backward retrieval, but this analysis did not indicate activation of any brain regions at a standard threshold of $p < .001$. In

contrast, when we contrasted backward retrieval versus forward retrieval, we observed activation of the left aVLPFC, left middle frontal gyrus, left inferior parietal lobule, and left postcentral gyrus (Table 1 and Fig. 3), indicating that the backward retrieval of sequentially organized episodic events require additional demands compared to the forward retrieval condition.

〈Table 1〉 Whole brain GLM analyses. Results of the retrieval runs from Phases 1

Regions	Hemisphere	BA	MNI Coordinates			*t*-score
			x	y	z	
Backward recall vs. Forward recall						
Inferior Frontal Gyrus	L	47	−48	39	−9	4.57
Middle Frontal Gyrus	L	6	−30	−9	66	4.72
	L	6	−39	6	63	4.04
Inferior Parietal Lobule	L	40	−39	−45	51	4.67
Postcentral Gyrus	L	3	−51	−18	60	3.96
	L	2	−57	−30	48	3.81
	L	2	−54	−30	57	3.81

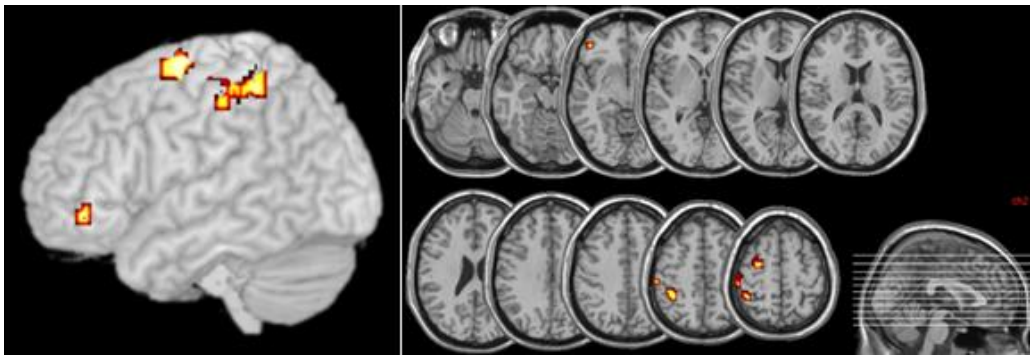

(Figure 3) General linear model analysis results. Contrast results for backward versus forward retrieval conditions

To ensure that the results obtained from this analysis did not mirror differences in the working memory load required, regions that overlapped with working memory results were excluded by subtracting the contrast results of 2-back versus 0-back (using a relaxed threshold, $p < .005$) from the overlapping map obtained above. The left aVLPFC (8 voxels) were remained after this analysis

was completed. These results are consistent with the prior findings that indicated the left aVLPFC played a crucial role in the controlled retrieval processes (Badre & Wagner, 2007).

Discriminating Temporal Retrieval Processes Using Patterns of Functional Connectivity

Given that GLM analyses did not provide information on inter-regional interactions but only indicated differential involvement of brain regions in sequential retrieval processes, we conducted intrinsic functional connectivity analysis using resting-state data to elucidate which neural regions were intrinsically connected each other. The left aVLPFC cluster as indicated by the GLM analyses was used as the seed region and interactivity (i.e., temporal correlations) of this region with the rest of the brain was assessed in a voxel-wise manner. The results showed a distributed connectivity maps encompassing the brain regions such as the bilateral superior frontal gyri, bilateral middle frontal gyri, bilateral inferior frontal gyri, bilateral medial frontal gyri, bilateral middle/inferior temporal gyri, bilateral caudate, and bilateral inferior parietal lobules (Table 2 and Fig. 4).

The intrinsic connectivity network map was then used to create a total of 31 nodes (See Section 2.6). To examine how these intrinsically connected brain regions (i.e., 31 nodes, Table 3 and Fig. 4) interacted with each other during temporal episodic memory task, we conducted fcMVPA using task-based time-series extracted from the retrieval run. Specifically, we used fcMVPA to investigate whether forward and backward retrieval processes recruited qualitatively different patterns of functional connectivity. The accuracy results obtained using fcMVPA are shown in Fig. 5. To investigate the number of features (i.e., functional connectivity between two different brain regions) required to produce optimally informative patterns in a classification algorithm, we performed a linear SVM pattern classification which iterated as a function of the number of features included. The SVM classification accuracies were 60% with only one feature and gradually increased to 87.5% when the top 91 features were included. The classification performance then gradually decreased and reached an accuracy of 57.5% when the complete set of features was included. To test whether the obtained peak accuracies were statistically different from the null distribution results, we conducted permutation testing which showed that accuracies remained near 50% demonstrating that the peak accuracies from the original data were derived from distinctive patterns of functional connectivity between the two different retrieval conditions (91 feature permutation mean = 0.49, SD = 0.12, C.I (95%) = 0.005; $p < .001$).

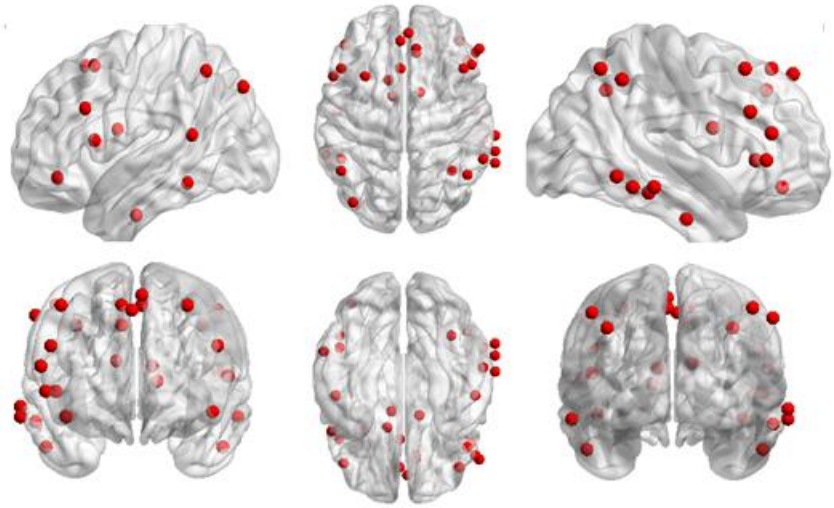

(Figure 4) Seed-selection based on resting-state analysis results. A total of 31 nodes (shown in red dots) obtained from the seed-based resting-state analysis. Each cube-shaped node was composed of 27 voxels centered on each peak voxel. Plotted nodes are spherical for visualization purposes and any voxels outside of the gray matter or image boundaries were excluded to obtain a representative time-series for each node. From top left in a clockwise direction: sagittal (left lateral), axial (top), sagittal (right lateral), coronal (back), axial (bottom), and coronal (front) views

The 91 features included in the peak accuracy were composed of functional connections among lateral and medial prefrontal regions, inferior parietal lobules, middle temporal gyrus, and caudate (Table 4 and Fig. 6). The interactivity patterns that discriminated between the two different sequential retrieval conditions encompassed regions that have been implicated in the cognitive control processes, such as the controlled memory retrieval regions (Badre & Wagner, 2007), the frontoparietal control network (Spreng, et al., 2010; Vincent, et al., 2008), the executive control network (Seeley, et al., 2007), and the goal-directed striatal region (Grahn, Parkinson, & Owen, 2008).

To understand the relative importance of each brain region in transferring information across the network, we computed the normalized betweenness centrality of each node included in the functional connectivity patterns that conferred peak classification accuracy. Betweenness centrality represents a node's centrality in a certain network and is computed as the total number of shortest paths between each pair of all other nodes that passes through the node (Freeman, 1977, 1978; Girvan & Newman, 2002). We computed the normalized betweenness centrality for each node by using the GraphVar

〈Table 2〉 Seed-based resting-state analysis. The left aVLPFC cluster was used as the seed region

Regions	Hemisphere	BA	MNI Coordinates			*t*-score
			x	y	z	
Seed-based						
Resting-state Analysis						
Inferior Frontal Gyrus*	L	47	-45	39	-9	671.91
*(Left anterior VLPFC, seed region)						
Superior Frontal Gyrus	R	8	9	36	54	4.64
	R	8	9	33	42	4.39
	R	9	3	48	51	4.06
	L	8	-3	42	60	4.05
Middle Frontal Gyrus	L	8	-30	15	54	12.15
	R	9	45	21	54	3.80
Inferior Frontal Gyrus	R	47	42	42	-12	17.08
	L	44	-54	15	12	13.10
	L	44	-48	21	30	12.70
	R	45	48	27	3	8.53
	R	45	54	33	3	7.71
	R	44	51	24	30	7.68
	R	45	57	36	18	7.18
Supplementary Motor Area	L	8	-3	21	54	9.62
Middle Temporal Gyrus	L	20	-60	-45	-12	11.05
	R	21	69	-30	-12	8.12
	R	20	60	-33	-15	7.45
	R	37	69	-51	-6	6.92
	L	37	-48	-48	15	4.87
Inferior Temporal Gyrus	L	20	-66	-30	-24	8.14
	R	20	63	-24	-33	7.50
	R	20	69	-42	-12	7.49
	L	20	-48	-6	-42	7.07
	R	20	69	-30	-24	6.89
	L	20	-51	-24	-36	6.23
	L	20	-60	-27	-33	5.66
	L	20	-54	-15	-39	5.31
	L	20	-51	-12	-30	4.95
	R	20	54	-6	-45	4.43
	R	20	63	-45	-27	4.35
	R	20	54	-12	-30	4.23
	R	20	45	-9	-39	4.11
Caudate	R	N/A	12	3	21	6.04
	L	N/A	-9	0	18	5.93
	L	N/A	-12	12	9	5.33
Inferior Parietal Lobule	L	40	-48	-57	51	15.41
	R	40	60	-48	48	7.37
Middle Occipital Lobule	L	19	-39	-81	42	5.66
Angular Gyrus	R	39	48	-60	54	7.46
	R	37	36	-57	-42	6.45
Fusiform Gyrus	R	20	39	-9	-45	4.37
Cerebellum	R	N/A	24	-81	-51	10.36
	R	N/A	36	-75	-48	8.19
	R	N/A	21	-69	-36	6.61
	L	N/A	-33	-72	-45	6.12
	L	N/A	-9	-84	-30	5.46
	R	N/A	12	-84	-27	5.22
	L	N/A	-24	-87	-51	4.45

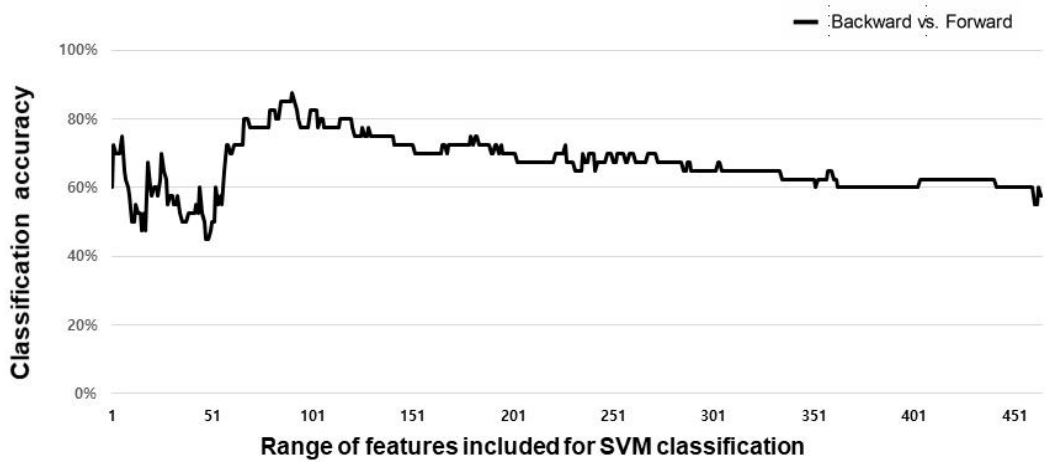

(Figure 5) Classification results for functional connectivity multivariate pattern analysis. The thick black lines represent the discrimination accuracies of the support vector machine (SVM) classifier (backward vs. forward retrieval) as a function of the range of features included. Peak accuracy of 87.5% was obtained when 91 features were included in the classification

toolbox (Kruschwitz, List, Waller, Rubinov, & Walter, 2015). The highly connected hub nodes with high betweenness centrality were located in the left caudates, right inferior parietal region, left inferior frontal, and inferior temporal lobule (see Table 3 last column for more node information and centrality degrees). Several high-ranked nodes were also located within the frontoparietal control network (Spreng, et al., 2010; Vincent, et al., 2008) and executive control network (Seeley, et al., 2007), such as the lateral prefrontal regions, inferior parietal lobules, and caudate.

fcMVPA Classification Performance across the Local Networks

To investigate how the decoding accuracy would change if a set of differently parsed functional networks are used, we repeat the decoding analyses using different sets of nodes. Specifically, we conducted this analysis to see whether functional connectivity patterns constructed with local brain regions would be informative in distinguishing between the temporally sequential retrieval processes. We parsed a total of 31 nodes into sets of local nodes based on the following criteria: 1) nodes located in the same hemisphere (hemispheric; left and right hemispheric) to investigate an effect associated with functional lateralization, 2) in the same regions (intra-lobular/-regional; frontal, temporal, parietal, and striatal region) to understand functional connectivity within each region is

〈Table 3〉 A total of 31 nodes generated from the seed-based resting-state connectivity analysis. Each node consists of 27 voxels (cube-shaped) and MNI coordinates represent the center of each node

Node #	Node Label	Hemisphere	MNI Coordinates			Centrality
			x	y	z	Betweenness
1	Inferior_Orbito_Frontal_L	L	-45	39	-9	2.76
2	Inferior_Frontal_Operculum_L	L	-54	15	12	1.88
3	Inferior_Frontal_Triangularis_L	L	-48	21	30	1.57
4	Middle_Frontal_L	L	-30	15	54	1.23
5	Supplimntary_Motor_Area_L	L	-3	21	54	1.16
6	Frontal_Sup_Medial_R_#1	R	9	36	54	1.16
7	Frontal_Sup_Medial_R_2	R	9	33	42	1.09
8	Frontal_Sup_Medial_R_#3	R	3	48	51	0.66
9	Frontal_Sup_Medial_L	L	-3	42	60	0.66
10	Inferior_Orbito_Frontal_R	R	42	42	-12	0.53
11	Inferior_Frontal_Triangularis_R_#1	R	48	27	3	0.27
12	Inferior_Frontal_Triangularis_R_#2	R	54	33	3	-0.19
13	Inferior_Frontal_Triangularis_R_#3	R	51	24	30	-0.23
14	Inferior_Frontal_Triangularis_R_#4	R	57	36	18	-0.26
15	Middle_Frontal_R	R	45	21	54	-0.28
16	Inferior_Parietal_L	L	-48	-57	51	-0.37
17	Middle_Occipital_L	L	-39	-81	42	-0.40
18	Middle_Temporal_L_#1	L	-48	-48	15	-0.56
19	Middle_Temporal_L_#2	L	-60	-45	-12	-0.62
20	Inferior_Temporal_L_#3	L	-51	-12	-30	-0.62
21	Middle_Temporal_R_#1	R	69	-30	-12	-0.66
22	Inferior_Temporal_R_#2	R	69	-42	-12	-0.74
23	Middle_Temporal_R_#3	R	60	-33	-15	-0.84
24	Middle_Temporal_R_#4	R	69	-51	-6	-0.86
25	Inferior_Temporal_R_#5	R	54	-12	-30	-0.89
26	Angular_R_#1	R	48	-60	54	-0.89
27	Inferior_Parietal_R	R	60	-48	48	-0.91
28	Angular_R_#2	R	36	-57	42	-0.91
29	Caudate_R	R	12	3	21	-0.91
30	Caudate_L_#1	L	-9	0	18	-0.91
31	Caudate_L_#2	L	-12	12	9	-0.91

Betweenness Centrality was Z scored.

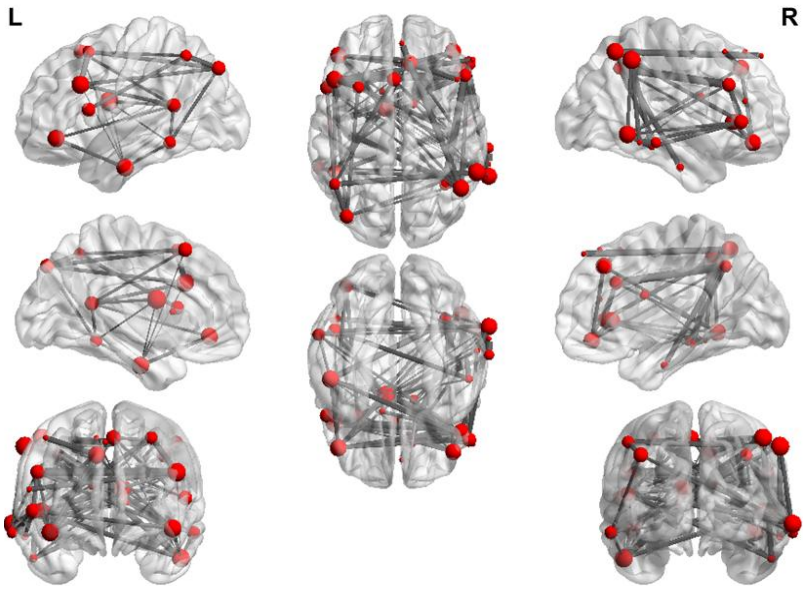

(Figure 6) Visualization of included features (edges between the two nodes shown in black lines) and nodes (shown in red dots) at the peak classification accuracies. Size of each circle (shown in red) is proportional to the normalized betweenness centrality value

sufficient for discriminating two different retrieval processes, and 3) across the two different regions (inter-lobular/-regional; fronto-temporal, fronto-parietal, and fronto-striatal) to explore which interactivity across two different brain areas is most informative in classification performance. Accuracies are depicted in Table 5. Mostly, SVM classification with cross-validation across the parsed local networks produced nearly chance level performance accentuating the original results obtained from the large-scale brain networks and iterative pattern classification analyses. The intra-lobular network within the temporal and parietal regions demonstrated slightly higher classification performance with maximum accuracy of 65% for both network. Nonetheless, the level of accuracy is numerically lower than the whole-brain large-scale network we constructed above. The current comparisons support our notion that large-scale consideration of whole brain connectivity is crucial to identify brain connections which are most informative in distinguishing different sequential retrieval conditions.

〈Table 4〉 Features that were included (edges between the two nodes) for peak accuracies

	Edge (Node #1 – Node #2)Feature rank	Mean *r*-value		*t*-value
		FR	BR	
1	'Caudate_L_#1~Inferior_Parietal_R'	0.13	0.34	2.40
2	'Middle_Temporal_L_#2~Inferior_Frontal_Triangularis_R_#1'	0.20	0.42	2.34
3	'Caudate_L_#1~Middle_Temporal_R_#4'	0.17	0.38	2.23
4	'Caudate_L_#1~Inferior_Temporal_R_#2'	0.16	0.35	2.22
5	'Caudate_L_#1~Angular_R_#1'	0.18	0.37	2.19
6	'Middle_Temporal_L_#2~Middle_Temporal_L_#1'	0.32	0.52	2.13
7	'Inferior_Orbito_Frontal_R~Frontal_Sup_Medial_R_#2'	0.38	0.52	2.08
8	'Inferior_Frontal_Triangularis_R_#2~Inferior_Orbito_Frontal_L'	0.36	0.52	2.07
9	'Middle_Temporal_R_#4~Inferior_Frontal_Triangularis_R_#1'	0.25	0.45	2.03
10	'Caudate_L_#1~Middle_Temporal_L_#2'	0.22	0.38	1.93
11	'Inferior_Parietal_R~Inferior_Orbito_Frontal_L'	0.27	0.42	1.92
12	'Inferior_Parietal_R~Inferior_Frontal_Triangularis_L'	0.13	0.32	1.83
13	'Caudate_L_#2~Inferior_Parietal_R'	0.17	0.33	1.80
14	'Caudate_L_#1~Inferior_Temporal_L_#3'	0.20	0.35	1.78
15	'Caudate_L_#1~Inferior_Frontal_Triangularis_R_#2'	0.29	0.44	1.77
16	'Inferior_Parietal_R~Supplimntary_Motor_Area_L'	0.17	0.34	1.77
17	'Middle_Temporal_L_#2~Middle_Occipital_L'	0.32	0.50	1.71
18	'Inferior_Parietal_R~Middle_Temporal_L_#2'	0.27	0.42	1.71
19	'Inferior_Parietal_R~Middle_Temporal_R_#4'	0.34	0.50	1.69
20	'Caudate_L_#1~Inferior_Frontal_Triangularis_R_#1'	0.30	0.44	1.68
21	'Middle_Temporal_R_#4~Inferior_Frontal_Triangularis_R_#3'	0.30	0.44	1.67
22	'Inferior_Orbito_Frontal_R~Inferior_Frontal_Triangularis_L'	0.22	0.40	1.65
23	'Middle_Temporal_R_#4~Middle_Temporal_L_#1'	0.37	0.52	1.64
24	'Caudate_L_#1~Inferior_Orbito_Frontal_R'	0.22	0.36	1.63
25	'Caudate_L_#1~Middle_Temporal_R_#3'	0.28	0.41	1.59
26	'Frontal_Sup_Medial_R_#2~Inferior_Orbito_Frontal_L'	0.26	0.40	1.58
27	'Inferior_Temporal_L_#3~Inferior_Frontal_Triangularis_L'	0.17	0.31	1.57
28	'Inferior_Frontal_Triangularis_R_#3~Inferior_Orbito_Frontal_R'	0.30	0.45	1.56
29	'Inferior_Frontal_Triangularis_R_#1~Inferior_Frontal_Triangularis_L'	0.33	0.44	1.55
30	'Middle_Temporal_R_#4~Inferior_Frontal_Triangularis_R_#2'	0.29	0.44	1.54
31	'Inferior_Temporal_R_#5~Middle_Temporal_L_#1'	0.43	0.32	1.50
32	'Caudate_R~Inferior_Temporal_R_#2'	0.19	0.32	1.50
33	'Inferior_Orbito_Frontal_R~Supplimntary_Motor_Area_L'	0.26	0.40	1.48

〈Table 4〉 Features that were included (edges between the two nodes) for peak accuracies (continued 1)

	Edge (Node #1 – Node #2)Feature rank	Mean *r*-value		*t*-value
		FR	BR	
34	'Caudate_R~Inferior_Temporal_L_#3'	0.19	0.32	1.48
35	'Angular_R_#1~Inferior_Temporal_R_#5'	0.50	0.37	1.48
36	'Middle_Temporal_R_#4~Supplimntary_Motor_Area_L'	0.17	0.31	1.46
37	'Middle_Temporal_L_#2~Inferior_Frontal_Triangularis_R_#2'	0.26	0.39	1.44
38	'Middle_Occipital_L~Inferior_Frontal_Triangularis_L'	0.36	0.48	1.44
39	'Middle_Temporal_R_#4~Frontal_Sup_Medial_R_#2'	0.32	0.45	1.44
40	'Middle_Frontal_L~Inferior_Frontal_Triangularis_L'	0.50	0.60	1.43
41	'Inferior_Orbito_Frontal_R~Middle_Frontal_L'	0.28	0.41	1.40
42	'Inferior_Frontal_Triangularis_R_#1~Inferior_Orbito_Frontal_R'	0.43	0.56	1.40
43	'Inferior_Frontal_Triangularis_R_#1~Inferior_Orbito_Frontal_L'	0.34	0.45	1.39
44	'Caudate_L_#1~Frontal_Sup_Medial_R_#1'	0.21	0.34	1.39
45	'Angular_R_#2~Inferior_Frontal_Triangularis_R_#3'	0.67	0.56	1.39
46	'Angular_R_#1~Frontal_Sup_Medial_R_#3'	0.57	0.47	1.35
47	'Inferior_Temporal_R_#2~Inferior_Frontal_Triangularis_R_#2'	0.27	0.40	1.34
48	'Inferior_Temporal_R_#2~Inferior_Frontal_Triangularis_R_#1'	0.32	0.44	1.33
49	'Inferior_Temporal_L_#3~Supplimntary_Motor_Area_L'	0.18	0.31	1.33
50	'Middle_Temporal_R_#4~Middle_Temporal_R_#3'	0.50	0.60	1.33
51	'Inferior_Temporal_L_#3~Inferior_Orbito_Frontal_L'	0.36	0.46	1.33
52	'Angular_R_#1~Inferior_Orbito_Frontal_L'	0.32	0.41	1.33
53	'Middle_Frontal_R~Frontal_Sup_Medial_R_#2'	0.48	0.35	1.32
54	'Inferior_Parietal_L~Supplimntary_Motor_Area_L'	0.33	0.42	1.30
55	'Inferior_Parietal_R~Middle_Temporal_R_#3'	0.45	0.54	1.29
56	'Middle_Temporal_L_#1~Inferior_Orbito_Frontal_L'	0.29	0.37	1.26
57	'Inferior_Parietal_L~Inferior_Frontal_Operculum_L'	0.37	0.25	1.26
58	'Middle_Temporal_L_#1~Supplimntary_Motor_Area_L'	0.31	0.43	1.25
59	'Inferior_Temporal_R_#2~Supplimntary_Motor_Area_L'	0.24	0.36	1.25
60	'Angular_R_#2~Inferior_Orbito_Frontal_L'	0.32	0.40	1.25
61	'Caudate_L_#1~Inferior_Frontal_Triangularis_R_#3'	0.50	0.57	1.25
62	'Frontal_Sup_Medial_L~Inferior_Frontal_Operculum_L'	0.23	0.12	1.24
63	'Angular_R_#1~Inferior_Temporal_L_#3'	0.52	0.42	1.23
64	'Angular_R_#1~Inferior_Frontal_Operculum_L'	0.26	0.17	1.23
65	'Middle_Temporal_R_#3~Inferior_Frontal_Triangularis_R_#2'	0.37	0.47	1.22

〈Table 4〉 Features that were included (edges between the two nodes) for peak accuracies (continued 2)

	Edge (Node #1 – Node #2)Feature rank	Mean *r*-value		*t*-value
		FR	BR	
66	'Inferior_Parietal_R~Inferior_Frontal_Operculum_L'	0.14	0.24	1.21
67	'Inferior_Temporal_L_#3~Frontal_Sup_Medial_R_#3'	0.50	0.41	1.21
68	'Angular_R_#1~Frontal_Sup_Medial_L'	0.56	0.47	1.21
69	'Inferior_Temporal_L_#3~Inferior_Frontal_Triangularis_R_#2'	0.37	0.46	1.20
70	'Inferior_Frontal_Triangularis_R_#3~Inferior_Frontal_Triangularis_L'	0.66	0.72	1.19
71	'Caudate_R~Middle_Temporal_R_#4'	0.23	0.33	1.18
72	'Inferior_Frontal_Triangularis_R_#3~Inferior_Frontal_Triangularis_R_#2'	0.44	0.54	1.18
73	'Inferior_Temporal_R_#2~Middle_Occipital_L'	0.31	0.44	1.16
74	'Inferior_Parietal_R~Inferior_Parietal_L'	0.49	0.57	1.16
75	'Inferior_Frontal_Triangularis_R_#3~Inferior_Orbito_Frontal_L'	0.34	0.43	1.16
76	'Inferior_Frontal_Triangularis_R_#4~Inferior_Frontal_Triangularis_L'	0.45	0.55	1.16
77	'Middle_Temporal_L_#1~Inferior_Frontal_Triangularis_L'	0.35	0.46	1.15
78	'Inferior_Temporal_L_#3~Middle_Temporal_L_#2'	0.30	0.42	1.15
79	'Inferior_Parietal_R~Inferior_Temporal_R_#2'	0.41	0.50	1.15
80	'Angular_R_#2~Middle_Temporal_R_#1'	0.40	0.30	1.15
81	'Caudate_L_#1~Inferior_Temporal_R_#5'	0.25	0.34	1.14
82	'Middle_Occipital_L~Inferior_Parietal_L'	0.46	0.56	1.14
83	'Caudate_L_#2~Inferior_Frontal_Triangularis_R_#1'	0.35	0.44	1.14
84	'Inferior_Temporal_L_#3~Inferior_Frontal_Triangularis_R_#1'	0.32	0.41	1.13
85	'Middle_Temporal_R_#1~Middle_Frontal_L'	0.43	0.31	1.13
86	'Inferior_Temporal_R_#2~Middle_Temporal_R_#1'	0.64	0.74	1.12
87	'Angular_R_#1~Inferior_Frontal_Triangularis_R_#2'	0.39	0.30	1.12
88	'Middle_Occipital_L~Middle_Frontal_L'	0.38	0.48	1.11
89	'Caudate_L_#1~Middle_Temporal_L_#1'	0.31	0.41	1.09
90	'Angular_R_#2~Inferior_Orbito_Frontal_R'	0.27	0.38	1.09
91	'Middle_Temporal_R_#4~Middle_Occipital_L'	0.27	0.38	1.08

Abbreviations: FR, forward retrieval; BR, backward retrieval; R, right hemisphere; L, left hemisphere.

〈Table 5〉 fcMVPA classification performance across separately parsed networks based on the following criteria; hemispheric, intra-lobular/-regional, and inter-lobular/-regional

Criteria	Network Label	Classification accuracy (%)	Included node #*
Hemispheric	Left hemisphere	40	1, 2, 3, 4, 5, 9, 16, 17, 18, 19, 20
	Right hemisphere	58	6, 7, 8, 10, 11, 12, 13, 14, 15, 21, 22, 23, 24, 25, 26, 27, 28, 29, 30
Intra-lobular/ -regional	Frontal lobe	53	1, 2, 3, 4, 5, 6, 7, 8, 9, 10, 11, 12, 13, 14, 15
	Temporal lobe	65	18, 19, 20, 21, 22, 23, 24, 25
	Parietal lobe	65	16, 26, 27, 28
	Striatal (caudate)	50	30, 31, 32
Inter-lobular/ -regional	Fronto-temporal	43	1, 2, 3, 4, 5, 6, 7, 8, 9, 10, 11, 12, 13, 14, 15, 18, 19, 20, 21, 22, 23, 24, 25
	Fronto-parietal	48	1, 2, 3, 4, 5, 6, 7, 8, 9, 10, 11, 12, 13, 14, 15, 16, 26, 27, 28
	Fronto-striatal	48	1, 2, 3, 4, 5, 6, 7, 8, 9, 10, 11, 12, 13, 14, 29, 30, 31

* Refer to Table 3.

Discussion

The aim of the current study was to elucidate patterns of functional connectivity associated with mnemonic control processes that were implicated in backward or forward retrieval of sequentially organized episodic events. We demonstrated that patterns of interactivity across a large-scale brain network constructed distinct functional connectivity structures during the two different directional retrieval conditions. Importantly, the multivariate pattern classification analyses using functional connectivity features reached great accuracy level, demonstrating that task-based interactivity of two sequential retrieval processes recruited qualitatively distinct network patterns. The iterative search methods embedded in machine learning algorithms revealed that discriminating patterns of connections include the interplay of the lateral and medial prefrontal regions, inferior parietal lobules, middle

temporal gyrus, and caudate, previously implicated in the cognitive control of memory and goal-directed cognitive process. We observed that connectivity patterns restricted to the locally parsed networks were not substantially effective in decoding the sequential retrieval processes.

Recently, functional connectivity analysis has been widely adopted to assess intrinsic or task-related interactivity across distributed brain regions. In contrast to the classical connectivity studies in which only bivariate seed-based connectivity has been applied to the resting-state scan or psychophysiological interaction (PPI) analysis, the advantages of multivariate pattern analysis approach based on the machine learning algorithm, especially using a large-scale task-based connectivity as input data, has recently been emphasized. For example, studies using task-related fMRI techniques have successfully utilized this approach for decoding neural responses during various cognitive tasks (Pantazatos, et al., 2012a, 2012b; Shirer, Ryali, Rykhlevskaia, Menon, & Greicius, 2012). In the present study, we applied the fcMVPA method to decode large-scale neural interactivity underlying controlled retrieval processes. Motivated by recent studies in which a novel fcMVPA approach had been applied (Pantazatos, et al., 2012a, 2012b), we gradually increased the number of features included with iteration of SVM classification processes, which resulted in a series of classification accuracies. With this protocol, we could monitor the changes in the pattern of accuracy as a function of the number of features included; and as a result, we were able to detect the features of functional connectivity that constructed the most informative patterns in distinguishing between the two different retrieval conditions.

The novel approach adopted in our methods was that we extracted condition-specific time-series instead of simple BOLD time-series for conducting functional connectivity analyses. To achieve this, we first extracted neural time-series across the whole retrieval runs and then convolved them with psychological factors (i.e., two different retrieval directions) to generate condition-weighted time-series in a voxel-by-voxel manner. Convolving neural time-series with psychological factors was originally used for generating interaction terms in the PPI functional connectivity approach (for a review see Friston, 2011; Friston, et al., 1997). In this method, researchers need to define one seed region to examine how other brain regions are functionally coupled with the predefined ROI. This poses a limitation in the number of seed regions, and the results from the PPI analysis represent a relationship only between the seed and other regions and not the interactivity across those regions. In contrast, fcMVPA allows us to examine how each brain region interacts with other areas within a large-scale brain network by simultaneously computing whole pair-wise cross-correlation coefficients.

Previous studies have shown intrinsic functional coupling between the lateral PFC regions and sub-cortical regions such as the caudate (Barnes, et al., 2010; Han, et al., 2012), and the results from the resting-state functional connectivity analysis in our study corroborate those earlier findings. More importantly, fcMVPA revealed functional coupling between these two regions during the task-state period and found that this link played an important role in distinguishing between sequential retrieval conditions. Given the role of the caudate region in guiding goal-directed behavior (Grahn, et al., 2008) and updating working memory (Marklund, et al., 2009), we predict that the right caudate will help participants hold the received cue item in the working memory, while the left aVLPFC supports successful backward retrieval in which a controlled retrieval process is required. During backward retrieval, fcMVPA results also illustrated that the left aVLPFC had functional connectivity with both the right inferior parietal lobule and the middle frontal gyrus. It is important to note that these regions are major components of the frontoparietal network (Spreng, et al., 2010; Vincent, et al., 2008). Converging neuroimaging evidence suggests that components of the frontoparietal network, including lateral PFC, anterior cingulate cortex, and inferior parietal lobule regions, play a crucial role in cognitive processes in which executive control is required (Badre & D'Esposito, 2007; Cabeza, et al., 2008; Corbetta, et al., 2008; Koechlin, et al., 1999). One plausible explanation for the observed functional coupling between the left aVLPFC and the parietal and middle frontal nodes in the current study is that the left aVLPFC actively engages in the cognitive control process to access goal-relevant episodic information, while the frontoparietal network supports a more general goal-directed cognitive process.

The univariate GLM analyses using the contrast of backward versus forward retrieval conditions enabled us to observe increased activation of the left aVLPFC. Moreover, this activation did not result from mere differences in the working memory load required between the two conditions, but rather from the demand required for controlled retrieval processes. If retrieval of the studied items backward simply required more working memory load than completing the task in the forward direction, we would expect to observe similar results as those of Sun et al. (2005). In their study, the authors demonstrated that backward recall processes compared to forward recall resulted in higher activity in the dorsolateral PFC (DLPFC, BA9), which indicated that backward recall requires more executive functions (see also D'Esposito, Postle, & Rypma, 2000 for a review). Alternatively, it is also possible that participants retrieve all items from the list simultaneously, regardless of the directional cue instructions, but then have difficulty selecting the correct answers among the competing alternatives,

especially in the backward conditions (Moss, et al., 2005; Thompson-Schill, D'Esposito, Aguirre, & Farah, 1997; Thompson-Schill, D'Esposito, & Kan, 1999). In contrast, participants may retrieve the forward target easily but need to actively search their stored memories in the backward conditions to restore their memory representations (Badre, et al., 2005; Han, et al., 2012; Wagner, et al., 2001). If the former account is correct, we would expect increased activation of mid-VLPFC, which has been implicated in domain-general selection processes that follow retrieval and resolve competition among many retrieved representations. Our results demonstrated the increased involvement of left aVLPFC during backward retrieval supporting the latter account consistent with controlled retrieval processes explanation.

Although we demonstrated the active involvement of several controlled network regions, it is important to note that informative patterns were not merely composed of connections with either positive or negative correlation coefficients. Importantly, the current findings using multivariate pattern analysis approach suggest that connections with various correlation strengths constructed the most informative patterns in distinguishing between forward and backward sequential retrieval processes. This is consistent with the idea that univariate analysis investigating the amplitude of a single region or bivariate seed-based connectivity analysis may not be adequate to capture the representation or underlying mechanism of complex cognitive processes, especially when the mechanisms involve the interaction of distributed nodes (i.e., Pantazatos, et al., 2012a). Nonetheless, the present study shows that the retrieval of sequentially organized episodic events in the backward direction requires increased involvement of the left aVLPFC, in which a controlled retrieval process has been implicated. Moreover, beyond the aVLPFC involvement did a successful retrieval of sequentially organized episodic events depend upon an interregional interactivity across a large-scale brain network, which has been implicated in goal-directed cognitive processes.

Conclusions

This study employed the fcMVPA approach to elucidate brain networks informative in distinguishing the backward retrieval process from the forward retrieval process. The results revealed that the large-scale functional connectivity patterns encompassing brain regions previously implicated in controlled retrieval process and goal-directed cognitive process, were substantially effective in decoding

the sequential retrieval processes (i.e., backward versus forward retrieval conditions). These findings suggest that the large-scale whole-brain networks are required during sequential retrieval processes of episodic memory, supporting the proposal that controlled processes across cortical and subcortical are recruited for the retrieval of temporal events and are mirrored in the patterns of functional connectivity.

Conflict of interest

The authors declare no competing financial interests.

References

Anders, T. R., & Lillyquist, T. D. (1971). Retrieval time in forward and backward recall. *Psychonomic Science, 22*, 205-206.

Badre, D., & D'Esposito, M. (2007). Functional magnetic resonance imaging evidence for a hierarchical organization of the prefrontal cortex. *Journal of Cognitive Neuroscience, 19*, 2082-2099.

Badre, D., Poldrack, R. A., Pare-Blagoev, E. J., Insler, R. Z., & Wagner, A. D. (2005). Dissociable controlled retrieval and generalized selection mechanisms in ventrolateral prefrontal cortex. *Neuron, 47*, 907-918.

Badre, D., & Wagner, A. D. (2007). Left ventrolateral prefrontal cortex and the cognitive control of memory. *Neuropsychologia, 45*, 2883-2901.

Barnes, K. A., Cohen, A. L., Power, J. D., Nelson, S. M., Dosenbach, Y. B., Miezin, F. M., Petersen, S. E., & Schlaggar, B. L. (2010). Identifying basal ganglia divisions in individuals using resting-state functional connectivity MRI. *Frontiers in Systems Neuroscience, 4*, 18.

Barredo, J., Oztekin, I., & Badre, D. (2015). Ventral fronto-temporal pathway supporting cognitive control of episodic memory retrieval. *Cerebral Cortex, 25*, 1004-1019.

Barredo, J., Verstynen, T. D., & Badre, D. (2016). Organization of cortico-cortical pathways supporting memory retrieval across subregions of the left ventrolateral prefrontal cortex. *J Neurophysiol, 116*, 920-937.

Cabeza, R., Ciaramelli, E., Olson, I. R., & Moscovitch, M. (2008). The parietal cortex and episodic

memory: an attentional account. *Nature Reviews Neuroscience, 9*, 613-625.

Corbetta, M., Patel, G., & Shulman, G. L. (2008). The reorienting system of the human brain: from environment to theory of mind. *Neuron, 58*, 306-324.

Cortes, C., & Vapnik, V. N. (1995). Support-vector networks. *Machine Learning, 20*, 273-297.

D'Esposito, M., Postle, B. R., & Rypma, B. (2000). Prefrontal cortical contributions to working memory: evidence from event-related fMRI studies. *Experimental Brain Research, 133*, 3-11.

Deichmann, R., Gottfried, J. A., Hutton, C., & Turner, R. (2003). Optimized EPI for fMRI studies of the orbitofrontal cortex. *Neuroimage, 19*, 430-441.

Dobbins, I. G., & Han, S. (2006). Cue- versus probe-dependent prefrontal cortex activity during contextual remembering. *Journal of Cognitive Neuroscience, 18*, 1439-1452.

Drosopoulos, S., Windau, E., Wagner, U., & Born, J. (2007). Sleep enforces the temporal order in memory. *PLoS One, 2*, e376.

Freeman, L. C. (1977). A set of measures of centrality based on betweenness. *Sociometry*, 35-41.

Freeman, L. C. (1978). Centrality in social networks conceptual clarification. *Social networks, 1*, 215-239.

Friston, K. J. (2011). Functional and effective connectivity: a review. *Brain Connect, 1*, 13-36.

Friston, K. J., Buechel, C., Fink, G. R., Morris, J., Rolls, E., & Dolan, R. J. (1997). Psychophysiological and modulatory interactions in neuroimaging. *Neuroimage, 6*, 218-229.

Friston, K. J., Glaser, D. E., Henson, R. N., Kiebel, S., Phillips, C., & Ashburner, J. (2002). Classical and Bayesian inference in neuroimaging: applications. *Neuroimage, 16*, 484-512.

Girvan, M., & Newman, M. E. (2002). Community structure in social and biological networks. *Proc Natl Acad Sci U S A, 99*, 7821-7826.

Grahn, J. A., Parkinson, J. A., & Owen, A. M. (2008). The cognitive functions of the caudate nucleus. *Progress in Neurobiology, 86*, 141-155.

Han, S., O'Connor, A. R., Eslick, A. N., & Dobbins, I. G. (2012). The role of left ventrolateral prefrontal cortex during episodic decisions: semantic elaboration or resolution of episodic interference? *Journal of Cognitive Neuroscience, 24*, 223-234.

Koechlin, E., Basso, G., Pietrini, P., Panzer, S., & Grafman, J. (1999). The role of the anterior prefrontal cortex in human cognition. *Nature, 399*, 148-151.

Kruschwitz, J. D., List, D., Waller, L., Rubinov, M., & Walter, H. (2015). GraphVar: a user-friendly toolbox for comprehensive graph analyses of functional brain connectivity. *J Neurosci Methods, 245*, 107-115.

Lezak, M. D. (1995). *Neuropsychological assessment*. New York: Oxford University Press.

Marklund, P., Larsson, A., Elgh, E., Linder, J., Riklund, K. A., Forsgren, L., & Nyberg, L. (2009).

Temporal dynamics of basal ganglia under-recruitment in Parkinson's disease: transient caudate abnormalities during updating of working memory. *Brain, 132*, 336-346.

Moss, H. E., Abdallah, S., Fletcher, P., Bright, P., Pilgrim, L., Acres, K., & Tyler, L. K. (2005). Selecting among competing alternatives: selection and retrieval in the left inferior frontal gyrus. *Cerebral Cortex, 15*, 1723-1735.

Neubert, F. X., Mars, R. B., Thomas, A. G., Sallet, J., & Rushworth, M. F. (2014). Comparison of human ventral frontal cortex areas for cognitive control and language with areas in monkey frontal cortex. *Neuron, 81*, 700-713.

Pantazatos, S. P., Talati, A., Pavlidis, P., & Hirsch, J. (2012a). Cortical functional connectivity decodes subconscious, task-irrelevant threat-related emotion processing. *Neuroimage, 61*, 1355-1363.

Pantazatos, S. P., Talati, A., Pavlidis, P., & Hirsch, J. (2012b). Decoding unattended fearful faces with whole-brain correlations: an approach to identify condition-dependent large-scale functional connectivity. *PLoS Computational Biology, 8*, e1002441.

Pantazatos, S. P., Talati, A., Schneier, F. R., & Hirsch, J. (2014). Reduced anterior temporal and hippocampal functional connectivity during face processing discriminates individuals with social anxiety disorder from healthy controls and panic disorder, and increases following treatment. *Neuropsychopharmacology, 39*, 425-434.

Pirogovsky, E., Goldstein, J., Peavy, G., Jacobson, M. W., Corey-Bloom, J., & Gilbert, P. E. (2009). Temporal order memory deficits prior to clinical diagnosis in Huntington's disease. *Journal of the International Neuropsychological Society, 15*, 662-670.

Raposo, A., Han, S., & Dobbins, I. G. (2009). Ventrolateral prefrontal cortex and self-initiated semantic elaboration during memory retrieval. *Neuropsychologia, 47*, 2261-2271.

Sagar, H. J., Sullivan, E. V., Gabrieli, J. D., Corkin, S., & Growdon, J. H. (1988). Temporal ordering and short-term memory deficits in Parkinson's disease. *Brain, 111*, 525-539.

Schofield, N. J., & Ashman, A. F. (1986). The relationship between digit span and cognitive processing across ability groups. *Intelligence, 10*, 59-73.

Seeley, W. W., Menon, V., Schatzberg, A. F., Keller, J., Glover, G. H., Kenna, H., Reiss, A. L., & Greicius, M. D. (2007). Dissociable intrinsic connectivity networks for salience processing and executive control. *Journal of Neuroscience, 27*, 2349-2356.

Shirer, W. R., Ryali, S., Rykhlevskaia, E., Menon, V., & Greicius, M. D. (2012). Decoding subject-driven cognitive states with whole-brain connectivity patterns. *Cerebral Cortex, 22*, 158-165.

Song, X. W., Dong, Z. Y., Long, X. Y., Li, S. F., Zuo, X. N., Zhu, C. Z., He, Y., Yan, C. G., & Zang, Y. F. (2011). REST: a toolkit for resting-state functional magnetic resonance imaging data

processing. *PLoS One, 6*, e25031.

Spreng, R. N., Stevens, W. D., Chamberlain, J. P., Gilmore, A. W., & Schacter, D. L. (2010). Default network activity, coupled with the frontoparietal control network, supports goal-directed cognition. *Neuroimage, 53*, 303-317.

Storandt, M., Kaskie, B., & Von Dras, D. D. (1998). Temporal memory for remote events in healthy aging and dementia. *Psychology and Aging, 13*, 4-7.

Sun, X., Zhang, X., Chen, X., Zhang, P., Bao, M., Zhang, D., Chen, J., He, S., & Hu, X. (2005). Age-dependent brain activation during forward and backward digit recall revealed by fMRI. *Neuroimage, 26*, 36-47.

Takahashi, E., Ohki, K., & Kim, D. S. (2007). Diffusion tensor studies dissociated two fronto-temporal pathways in the human memory system. *Neuroimage, 34*, 827-838.

Thomas, J. G., Milner, H. R., & Haberlandt, K. F. (2003). Forward and backward recall: different response time patterns, same retrieval order. *Psychological Science, 14*, 169-174.

Thompson-Schill, S. L., D'Esposito, M., Aguirre, G. K., & Farah, M. J. (1997). Role of left inferior prefrontal cortex in retrieval of semantic knowledge: a reevaluation. *Proceedings of the National Academy of Sciences, U.S.A., 94*, 14792-14797.

Thompson-Schill, S. L., D'Esposito, M., & Kan, I. P. (1999). Effects of repetition and competition on activity in left prefrontal cortex during word generation. *Neuron, 23*, 513-522.

Tulving, E. (1972). Episodic and semantic memory. In E. Tulving & W. Donaldson (Eds.), *Organization of memory* (pp. 381-403). New York: Academic Press.

Tulving, E. (1983). *Elements of episodic memory*. Oxford: Clarendon Press.

Tulving, E. (2002). Episodic memory: from mind to brain. *Annual Review of Psychology, 53*, 1-25.

Vapnik, V. N. (1999). An overview of statistical learning theory. *IEEE Transactions on Neural Networks, 10*, 988-999.

Vincent, J. L., Kahn, I., Snyder, A. Z., Raichle, M. E., & Buckner, R. L. (2008). Evidence for a frontoparietal control system revealed by intrinsic functional connectivity. *Journal of Neurophysiology, 100*, 3328-3342.

Vriezen, E. R., & Moscovitch, M. (1990). Memory for temporal order and conditional associative-learning in patients with Parkinson's disease. *Neuropsychologia, 28*, 1283-1293.

Wagner, A. D., Pare-Blagoev, E. J., Clark, J., & Poldrack, R. A. (2001). Recovering meaning: left prefrontal cortex guides controlled semantic retrieval. *Neuron, 31*, 329-338.

Wechsler, D. (2008). *Wechsler adult intelligence scale–fourth edition (WAIS–IV)*. San Antonio: NCS Pearson.

Yan, C. G., & Zang, Y. F. (2010). DPARSF: a MATLAB toolbox for "pipeline" data analysis of

resting-state fMRI. *Frontiers in Systems Neuroscience, 4*, 13.

1차 원고 접수: 2018. 06. 11
1차 심사 완료: 2018. 07. 16
2차 원고 접수: 2018. 07. 23
2차 심사 완료: 2018. 07. 23
최종 게재 확정: 2018. 08. 08

(요 약)

시간적 일화기억인출에 관여하는 뇌기능연결성 연구

나 윤 진[1)] 이 종 현[2)] 한 상 훈[1),2)]

[1)]연세대학교 심리학과

[2)]연세대학교 인지과학 협동과정

부호화된 사건의 시간적 정보를 기반으로 한 인출은 일화기억의 중요한 통제기제 중 하나이다. 기억인출과 관련한 수많은 신경영상 연구들이 진행되었음에도 아직 시간적으로 구성된 일화기억의 인출에 관여하는 뇌신경연결망 패턴에 대해서는 알려진 바가 많지 않다. 본 연구에서는 두가지 다른 순차적 인출 뇌신경 기제를 구분하기 위하여 과제기반 기능적 연결성 다변량 패턴분석 방법을 사용하였다. 참가자들은 시간적 일화기억과제를 수행하였고, 순서대로 부호화된 기억자극을 순방향 혹은 역방향으로 인출하도록 지시를 받았다. 부분적으로 분류된 국소적 신경네트워크 패턴은 두 인출기제를 잘 구분하지 못한 반면, 기억과 관련된 인지통제 영역과 목표-지향적 인지기제처리에 관련된 것으로 알려진 여러 피질-피질하 노드들을 아우르는 전뇌신경네트워크 패턴은 시간적 일화기억 인출기제를 잘 구분하였다. 이 영역들은 측면/내측 전전두엽 영역, 하부 두정엽, 중간 측두회, 선조체 영역 등을 포함하며 기계학습을 이용한 분류에서 높은 분류 예측률을 보였다. 본 연구의 결과는 일화기억의 시간적 인출기제에 관여하는 피질-피질하 여러 영역의 관여를 확인하였고, 대역적 네트워크 패턴의 기능적 연결성이 질적으로 다른 인출기제에 관여함을 확인하였다는데에 중요성을 갖는다.

주제어 : 통제된 인출, 기능적 연결성, 다변량패턴분석, 시간적 일화기억